JOURNAL OF MATERIALS SCIENCE 26 (1991) 1659–1665

Study of cracking and microstructural evolution during drying of tape-cast aluminium nitride sheets

E. STREICHER, T. CHARTIER
UA CNRS 320-ENSCI, 47173 AV. Albert Thomas, F-87065 Limoges, France
P. BOCH
ESPCI, 10 Rue Vauquelin, F-75231 Paris, France

The influence of organic phases on the drying of tape-cast aluminium nitride green sheets was studied. The cracking during drying and the microstructure of green tapes are sensitive to the inorganic to organic and binder to plasticizer ratios. A high amount of a plasticizer-rich organic phase promotes a low-speed shrinkage of the green tape during drying and prevents it from cracking. The apparent density and the porosity of the green tapes decrease whereas the total shrinkage of the green tapes increases when the organic content increases. The apparent density increases whereas the porosity and the shrinkage decrease when the plasticizer content increases.

1. Introduction

Large and thin ceramic pieces are generally processed by tape-casting [1]. Tape-casting slurries are composed of ceramic powders dispersed in a solvent with dispersant, binder and plasticizer additions. Each composition must be adjusted according to the powder characteristics, the thickness of the tape and other processing parameters (not only casting parameters but also thermocompression, pyrolysis and sintering ones). Fiori and DePortu [2] suggest some rules for the preparation of a tape-casting slurry, namely (i) the plasticizer to binder ratio must be less than 2, (ii) the amount of dispersant must be chosen in the range where the adsorption is constant, (iii) the ratio between organic components and ceramic powder must be as low as possible, and (iv) the amount of solvent must be fixed at the minimum to ensure a good dissolution of organic components and a good homogenization of the slurry. An optimized slurry leads to tapes which satisfy most of the following criteria: (i) no cracking during drying, (ii) a good cohesion to allow the manipulation of the dried sheets, (iii) a good microstructural homogeneity, (iv) a good thermocompression ability, and (v) an easy pyrolysis.

The optimization of the tape-casting slurry requires a close control of numerous parameters, in particular those related to the cracking during drying. The present work studies the drying behaviour in air of aluminium nitride tape-cast sheets. The relations between the evaporation of the solvent and the shrinkage of the tape with its cracking are determined. The evolution of the microstructure (porosity) of tapes during drying is also determined. The influence of the nature and amount of the organic components as well as the influence of the mean grain size of the ceramic powder are evaluated.

2. Experimental procedure

2.1. Starting materials

The aluminium nitride powders (Starck, Germany) were of three grades (A, B and C) with a mean grain size of 8, 2 and 1.3 μm, respectively. An yttrium oxide powder (Rhone-Poulenc, France) with a mean grain size of 8.5 μm was chosen as sintering aid.

The solvent was an azeotropic mixture of 66/34 vol % butanone 2/ethanol. The dispersant was a phosphate ester (C213, CECA, France). The binder was a polyvinyl butyral (PVB). The plasticizer was a 50/50 wt % mixture of polyethylene glycol (PEG) and phthalate (PHT).

2.2. Sample preparation

Three parameters were chosen for the study. The first was the inorganic to organic ratio (X), equal to the volume of powder divided by total volume of powder, dispersant, binder and plasticizer. The second parameter was the binder to plasticizer ratio (Y), equal to the volume of binder divided by the volume of plasticizer. The third parameter was the mean grain size of the ceramic powder: 8, 2 and 1.3 μm for A, B and C grades, respectively. The slurry compositions are given in Tables I and II. The C_{o3} composition (Table I) is used to study the influence of grain size. Green sheets with a thickness of 200 to 300 μm were tape-cast on glass supports. The drying rate was evaluated on green sheets 20 cm long. The cracking of the tapes was detected visually using samples 1 m long. In all cases, the viscosity was kept at 800 mPa sec by adjusting the amount of solvent.

2.3. Characterization

The sheets stick on to the surface of the support during drying. As the glass support is rigid, we can suppose

0022–2461/91 $03.00 + .12

TABLE I Slurry compositions for various X ratios

Component	Density ($g\,cm^{-3}$)	Composition (vol %)				
		C_{o1}	C_{o2}	C_{o3}	C_{o4}	C_{o5}
AlN (B)	3.16	38.53	33.89	33.09	29.77	23.45
Y_2O_3	4.7	0.79	0.70	0.69	0.62	0.48
C-213	1.05	0.25	0.22	0.22	0.20	0.16
Solvent	0.8	52.86	54.60	53.25	53.27	55.96
PVB	1.1	3.35	4.67	5.61	7.14	8.82
PHT	1.05	2.19	3.06	3.68	4.67	5.77
PEG	1.13	2.03	2.85	3.42	4.33	5.36
X		0.83	0.76	0.72	0.65	0.54
Y				0.79		

TABLE II Slurry compositions for various Y ratios

Component	Composition (vol %)			
	C_{b1}	C_{b2}	C_{b3}	C_{b4}
AlN (B)	39.47		33.89	
Y_2O_3	0.81		0.70	
C-213	0.26		0.22	
Solvent	47.09		54.59	
PVB	2.82	4.68	6.34	7.00
PHT	4.94	3.07	2.19	1.83
PEG	4.59	2.84	2.04	1.70
Y	0.30	0.79	1.50	1.98
X		0.76		

that the shrinkage operates mostly in the thickness direction, perpendicular to the surface of the tape. The shrinkage of the tape during drying is measured by a laser method (Fig. 1). The laser beam is focused on the tape surface and we get an A′ image of point A on a screen (Fig. 1a). If the tape shrinks, the laser beam is no longer focused on A and the A′ point grows to an A′B′ spot (Fig. 1b). The shrinkage is equal to the displacement of the lens to achieve a new focalization. The evaporation of the solvent is measured simultaneously by a balance connected to a computer. Two measurements of shrinkage and weight are performed for each composition.

The shrinkage (S) is calculated as the ratio S_t/T_f where S_t is the shrinkage at time t and T_f the final thickness of the tape after complete drying. Using the least-squares method, the evolution of the shrinkage with the drying time was approximated by the relation:

$$S(t) = a_1 e^{b_1/t}$$

where a_1 and b_1 are constants. The shrinkage rate (SR) is calculated by differentiation of the above relation:

$$SR(t) = \frac{T_f dS(t)}{dt} = -\frac{T_f a_1 e^{b_1/t} b_1}{t^2}$$

The remaining amount of solvent (RS) is given by

$$RS = \frac{W_t - W_f}{W_o - W_f}$$

where W_t is the weight of the tape at time t; W_o and W_f are the initial and final weight of the tape. A two-stage process is commonly observed for the drying of green tapes [3, 4]. Empirically, it is observed that the first stage of drying proceeds at a constant rate, so a convenient expression of the residual fraction of solvent is

$$RS(t) = a_2 t + b_2$$

where a_2 and b_2 are constants. For a longer time, the evaporation rate decreases exponentially and a convenient expression is

$$RS(t) = a_3 e^{b_3/t}$$

where a_3 and b_3 are constants. The drying rate (DR) is calculated for each time (t_i) using the relation

$$DR(t_i) = \frac{W(t_{i-1}) - W(t_i)}{t_{i-1} - t_i}$$

The variations of weight and shrinkage with time allow the calculation of the volumic fraction of each component of the tape during drying (powder, organic phase, porosity). The assumption is that the total volume is the sum of the volumes of powder, organic phase and porosity. Negative values of the porosity are sometimes obtained because of the imprecision of the thickness measurement.

The apparent density, excluding the organic phase, of green samples was determined by measuring the volume and weight of samples before and after calcination (V and V_{cal} for the volume, M and M_{cal} for the weight). Apparent density was expressed by the ratio M_{cal}/V.

3. Results and discussion

3.1. Cracking during drying

Cracking occurs in green tapes when the B grade is used for $X > 0.76$ (Table III). As far as Y is concerned, cracking develops in B-grade tapes for $Y > 0.79$ (Table IV). When a C_{03} composition with A, B and C grades is cast, cracking only appears in the C-grade tapes.

3.2. Shrinkage and evaporation

Whatever the composition and powder grade, the evolutions of shrinkage (S) and evaporation (RS) during drying are similar. Examples of these evolutions for C_{01}, C_{b1} (B grade) and C_{03} (B and C grades) compositions are shown in Fig. 2. The first stage of

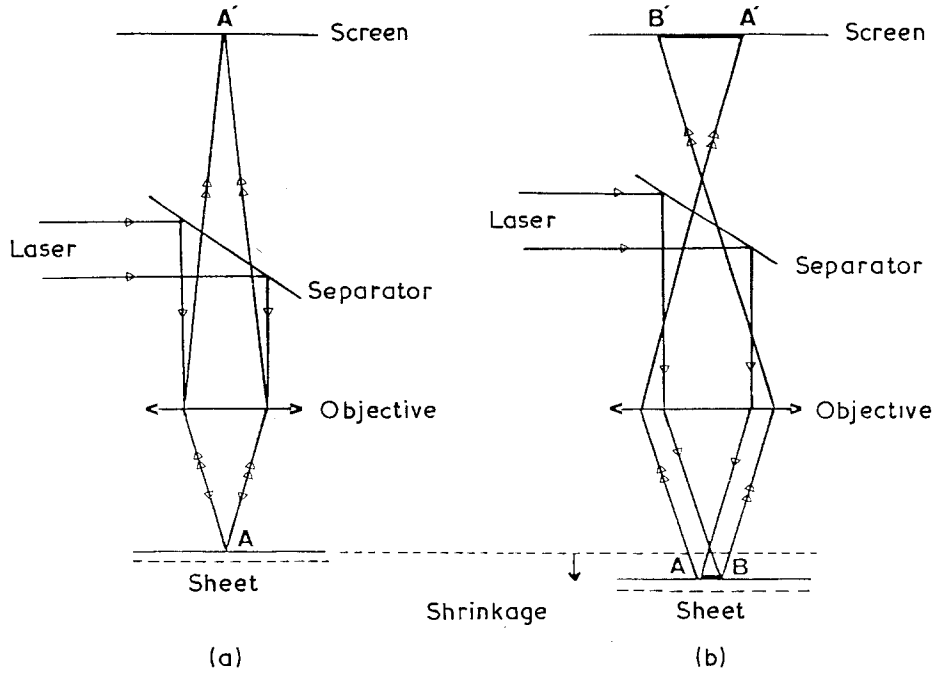

Figure 1 (a, b) Schematic diagrams of the shrinkage measurement device.

TABLE III Cracking during drying (X ratio)

Composition	No cracks	Slightly cracked	Cracked
C_{o1}			X
C_{o2}	X		
C_{o3}	X		
C_{o4}	X		
C_{o5}	X		

TABLE IV Cracking during drying (Y ratio)

Composition	No cracks	Slightly cracked	Cracked
C_{b1}	X		
C_{b2}	X		
C_{b3}		X	
C_{b4}			X

the evaporation process at constant rate is not observed for our slurry compositions at room temperature in air.

The drying rate continuously decreases with time; this behaviour does not depend on the composition of the slurry and the grade of powder (Fig. 3). On the other hand, the shrinkage rate presents a maximum value which depends on the slurry parameters (X, Y and granulometry of the powder) (Fig. 4 and Table V). The shrinkage rate increases when X or Y increases. A smaller grain size of the powder also increases the shrinkage rate.

3.3. Microstructural features

The calculation of the volumic fractions of each component (powder, solvent, organic phase and porosity) allows one to understand the evolution of the microstructure of the tape during drying. This study is focused on porosity, which is the most significant parameter. The value of porosity is more than 0% at the initial time of drying (i.e. just after casting) and values as high as 20% are calculated. At the beginning of drying, during shrinkage, the porosity decreases to a minimum (generally 0%) and then increases.

Table VI presents the shrinkage, apparent density and porosity of dried tapes with various X ratios. When X increases, the apparent density and the final porosity of the tapes increase, while the total shrinkage decreases. Fig. 5 shows the evolution of porosity with drying time for various X-ratio compositions. Low X ratios cause a slower porosity rate decrease: when $X \geqslant 0.76$, the porosity decreases to a minimum value after 3 to 4 min, while 10 to 12 min are necessary to obtain the minimum of porosity when $X \leqslant 0.72$. In addition, when the X ratio is high ($\geqslant 0.76$), the porosity does not disappear completely during shrinkage; about 8% remains at the minimum for the C_{o1} composition ($X = 0.83$).

Table VII gives the final characteristics of dried tapes with various Y ratios. When Y increases the apparent density decreases while porosity and total shrinkage increase. Fig. 6 shows the evolution of porosity with time for various Y-ratio compositions. For the lowest Y ratio ($Y = 0.3$), the initial porosity does not disappear completely and a porosity of about 7% remains at the minimum for the C_{b1} composition.

Table VIII displays the final characteristics of C_{o3} composition dried tapes made of A, B and C grades. The highest value of density with the lowest value of porosity is obtained for B-grade tapes. The total shrinkage value is a maximum for the C grade. Fig. 7 shows the evolution of porosity with the drying time for the three AlN grades. Whatever the grade, the evolutions of porosity are similar. Porosity decreases to 0% after 3 to 8 min of drying time and then increases up to 20 to 29% after complete drying.

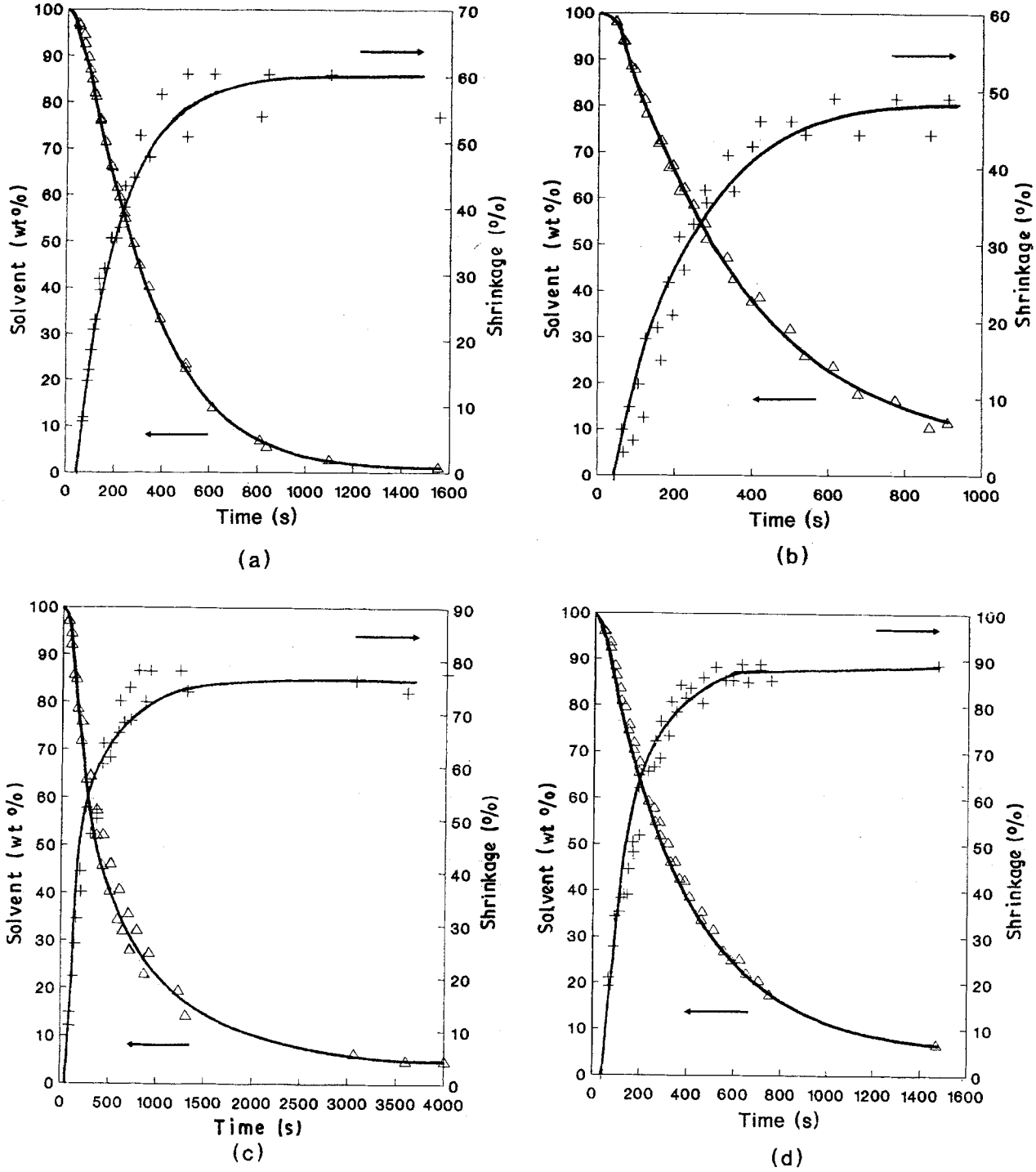

Figure 2 (Δ) Evaporation of solvent and (+) shrinkage during drying: (a) C_{o1}, (b) C_{b1} compositions of B grade; and C_{o3} composition of (c) B grade and (d) C grade.

3.4. Influence of drying behaviour on fissuration

The drying of tape-cast sheets has been studied by Shanefield [3] and Mistler *et al.* [4]. A two-stage process is commonly observed. In the first stage, the slurry is still fluid and the solvent flows through the sheet by liquid diffusion or capillary action and evaporates at the surface at a constant rate. In the second stage, the surface of the sheet becomes solid and the slow diffusion of the solvent reduces the drying rate. Stresses develop in the sheet due to the migration of the solvent and to the shrinkage. Fig. 8 schematizes the stresses due to shrinkage in a dried tape. The surface dries first and then the centre: compression stresses develop inside the centre and tension stresses at the surface. When the end of the shrinkage occurs during the first stage of evaporation, stresses due to shrinkage (first-stage evaporation) and evaporation (second-stage evaporation) do not overlap. On the other hand, when the end of shrinkage occurs during the second stage of evaporation the two stresses overlap, and cracking may easily occurs.

In our experimental conditions (i.e. room temperature, air drying, 250 μm tape thickness), we only observe one stage of evaporation which refers to a second stage. The drying rate continuously decreases with time. The first stage is probably too short to be detected. So, whatever the composition, the end of

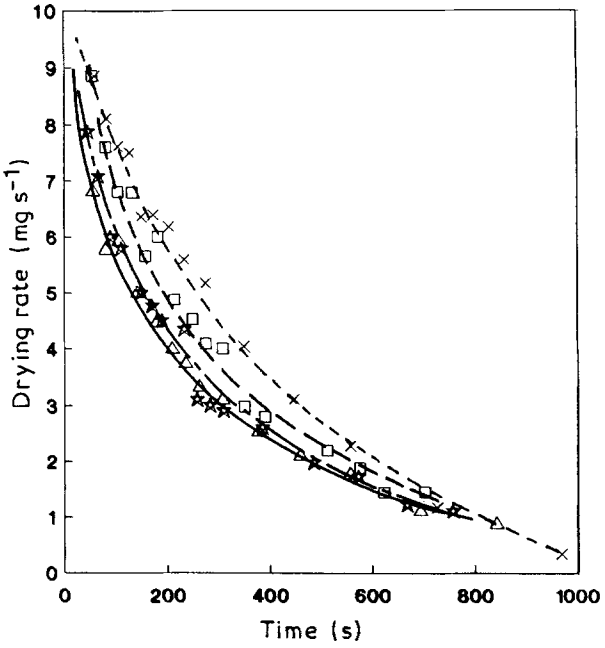

Figure 3 Drying rate against time for (X, – – –) C_{o1}, B grade; (Δ, ——) C_{b1}, B grade; (☆, –.–) C_{o3}, B grade; (□, – –) C_{o3}, C grade.

shrinkage occurs during the second stage, and, according to the above analysis, there is a high cracking risk. Our study shows that cracking is dependent on the shrinkage rate which itself depends on the slurry composition. For low-X compositions, the organic phase slows down the grain motion and the rate of shrinkage (which is due to grain rearrangements) decreases. The binder ensures the cohesion of the green tapes by bonding the mineral particles. When the amount of binder increases (high Y ratio) the links between the particles become stronger and the shrinkage rate increases. To avoid fissuration a low speed of shrinkage must be obtained, requiring compositions with (i) a low X ratio (high amount of organic components), (ii) a low Y ratio (high amount of plasticizer), and (iii) a medium mean grain-size ceramic powder.

TABLE V Evolution of the maximum of shrinkage rate for various X and Y ratios and for the three AlN grades

Parameter studied	Maximum shrinkage speed (μm sec^{-1})
X (Y = 0.79)	
0.83	0.88
0.76	0.83
0.72	0.78
0.65	0.80
0.54	0.79
Y (X = 0.76)	
0.30	0.61
0.79	0.83
1.50	0.88
1.98	1.13
AlN grade	
A	0.77
B	0.78
C	1.35

3.5. Evolution of porosity during drying

After casting, the porosity of the tape is not equal to zero. This porosity is probably due to air bubbles trapped in the green sheet. Then, after casting, grain rearrangement occurs and the bubbles burst on the surface of the sheet. The porosity decreases until the end of the shrinkage. The subsequent evaporation of the remaining solvent creates the final porosity of the dried green sheet.

Fig. 9 shows the influence of the X ratio on the microstructure of the green sheets. When X decreases, the organic phases prevent ceramic particles from packing together. The density decreases but porosity decreases simultaneously (Table VI). The porosity is filled by organic components [5]. The evolution of the

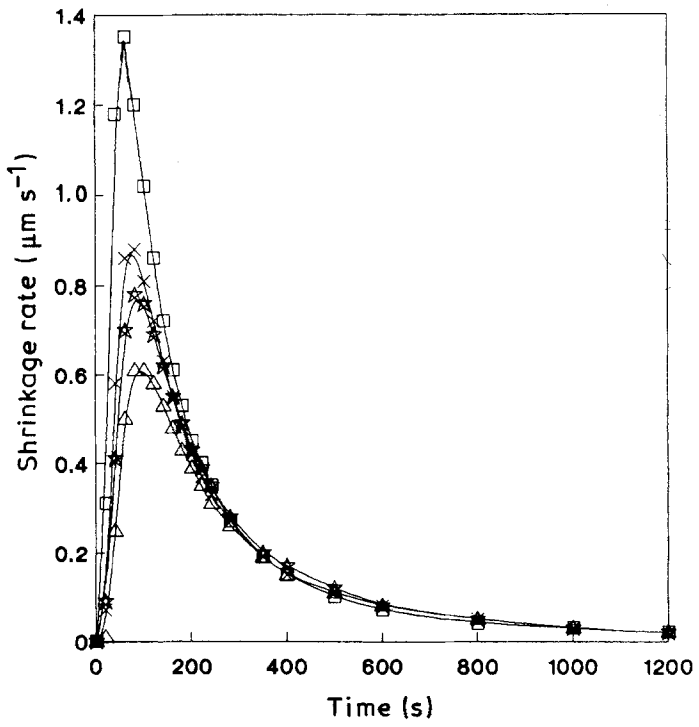

Figure 4 Shrinkage rate against time for (X, – – –) C_{o1}, B grade; (Δ, —) C_{b1}, B grade; (☆, –.–) C_{o3}, B grade; (□, – –) C_{o3}, C grade.

TABLE VI Total shrinkage, apparent density and porosity of dried green sheets for various X ratios

Composition	Total shrinkage (%)	Density (g cm^{-3})	Porosity (vol %)
C_{o1}	0.57	1.98	26
C_{o2}	0.70	1.90	21
C_{o3}	0.76	1.87	20
C_{o4}	1.16	1.79	14
C_{o5}	1.40	1.66	4

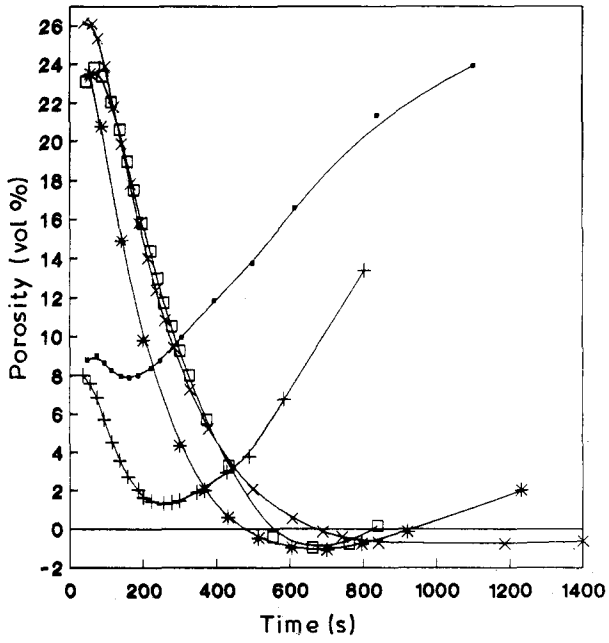

Figure 5 Porosity against time for various X ratios: (■) C_{o1}, $X = 0.83$; (+) C_{o2}, $X = 0.76$; (*) C_{o3}, $X = 0.72$; (□) C_{o4}, $X = 0.65$; (X) C_{o5}, $X = 0.54$.

TABLE VII Total shrinkage, apparent density and porosity of dried green sheets for various Y ratios

Composition	Total shrinkage (%)	Density (g cm^{-3})	Porosity (vol %)
C_{b1}	0.46	1.99	19
C_{b2}	0.70	1.90	21
C_{b3}	0.80	1.83	25
C_{b4}	0.92	1.81	26

TABLE VIII Total shrinkage, apparent density and porosity of dried green sheets of various AlN grades for the C_{o3} composition

AlN grade	Total shrinkage (%)	Density (g cm^{-3})	Porosity (vol %)
A	0.66	1.77	29
B	0.76	1.87	20
C	0. 87	1. 83	23

tape's porosity with time depends on the X ratio. The shrinkage rate decreases when X decreases. So, for low-X slurries, the removal of the porosity is delayed. In addition, for high X values, the mineral particles are close to one another and their respective motions are too small (total shrinkage decreases when X

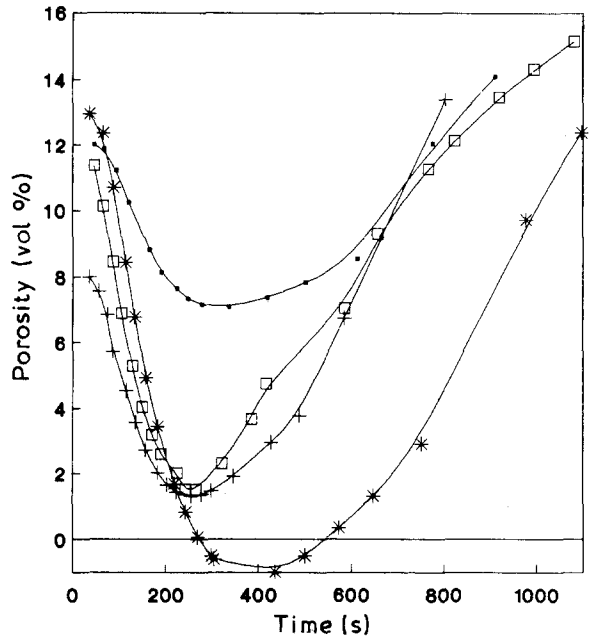

Figure 6 Porosity against time for various Y ratios: (■) C_{b1}, $Y = 0.3$; (+) C_{b2}, $Y = 0.79$; (*) C_{b3}, $Y = 1.5$; (□) C_{b4}, $Y = 1.98$.

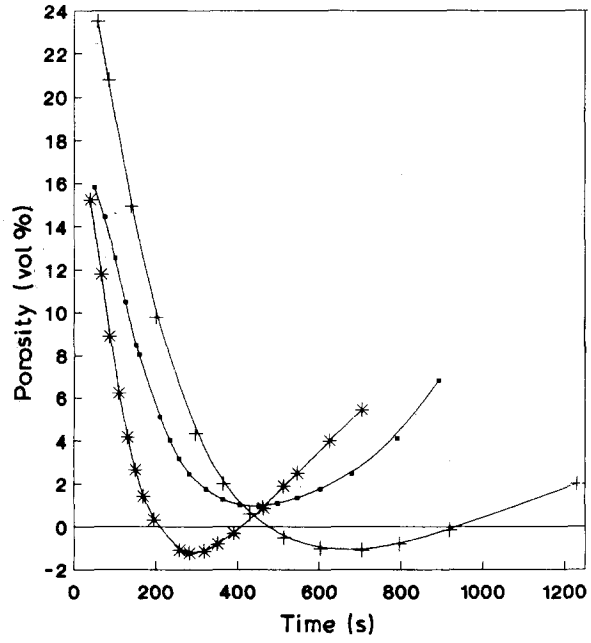

Figure 7 Porosity against time for (■) A, (+) B and (*) C grades (C_{o3} composition).

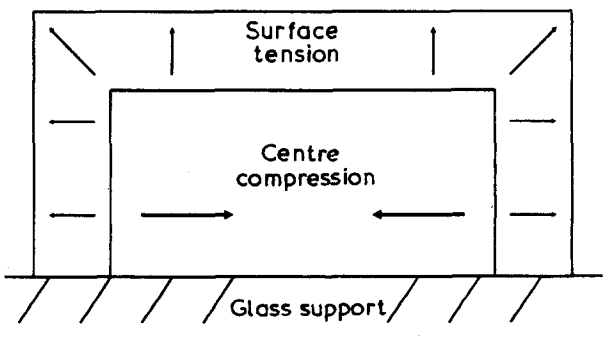

Figure 8 Schematic diagram of stresses which develop during drying.

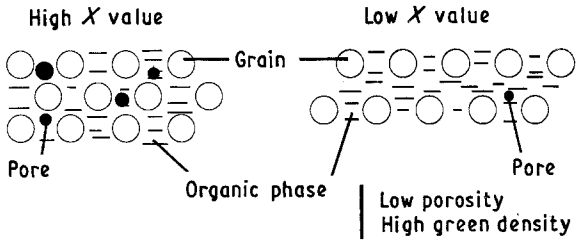

Figure 9 Influence of X ratio on the microstructure of the green sheets.

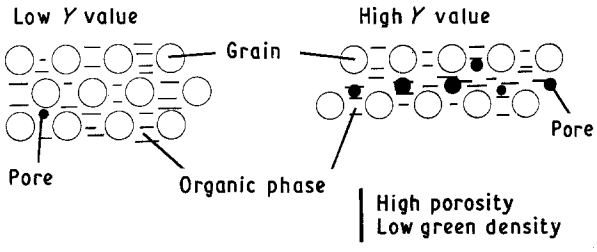

Figure 10 Influence of Y ratio on the microstructure of the green sheets.

increases) to allow a complete elimination of the porosity.

Fig. 10 shows the influence of the Y ratio on the microstructure of green sheets. A low Y ratio leads to green tapes with higher density and lower porosity than high-Y ones. When the Y ratio decreases, the porosity of the tapes decreases but its elimination is not complete during the early drying. In that case again, the grain rearrangement is too small to allow a complete removal of the porosity. Nevertheless, after shrinkage, the very low-viscosity plasticizer-rich organic phase may flow between the grains and fill the porosity, leading to the lowest-porosity samples.

AlN B leads to green products with higher densities than those using A and C grades. The same results have been obtained with dry pressed samples without any organic component: 1.82, 1.92 and 1.89 g cm^{-3} for AlN A, B, C, respectively, for a pressure of 160 MPa. Powders with a coarse or too-small mean grain size are generally difficult to compact. The evolution of porosity with time is not sensitive to mean grain size.

4. Conclusion

This study has shown that the organic phase of a tape-casting slurry greatly influences cracking during drying and the microstructure of green tapes. Slurry compositions with various inorganic to organic ratios (X) and various binder to plasticizer ratios (Y) were studied.

A high apparent density requires a high value of X, whereas a low volume of pores and a high resistance to fissuration (low speed of shrinkage) are obtained for a low value of X.

A high apparent density, a low volume of pores and a high resistance to cracking require a low value of Y.

A medium mean grain size (i.e. 2 μm) of the AlN powder leads to (i) a high value of green density, (ii) a low value of porosity, and (iii) a low speed of shrinkage.

References

1. E. P. HYATT, *Amer. Ceram. Soc. Bull.* **65** (1986) 637.
2. C. FIORI and G. De PORTU, *Br. Ceram. Proc.* **38** (1986) 213.
3. D. J. SHANEFIELD, in "Encyclopedia of Materials Science and Engineering", edited by M. B. Bever (Pergamon, New York, 1983) pp. 4855–4858.
4. R. E. MISTLER, D. J. SHANEFIELD and R. B. RUNK, in "Ceramic Processing before Firing", edited by G. Y. Onada and L. L. Hench (Wiley, New York, 1978) pp. 411–447.

Received 19 December 1989
and accepted 2 August 1990